Molecular Motions of Poly(ethyl acrylate) and Poly(*n*-butyl acrylate) Studied by Solid-State NMR and Molecular Dynamics Computer Experiments

Hiroaki Kikuchi,* Hideyuki Tokumitsu, and Kazuhiko Seki

Second Research Department, NOK Corporation, 25 Wadai, Tsukuba-shi, Ibaraki, 300-42 Japan

Received November 13, 1992; Revised Manuscript Received September 14, 1993•

ABSTRACT: The ^{13}C spin–lattice relaxation time (T_1^C) has been measured for bulk poly(ethyl acrylate) (PEA) and poly(*n*-butyl acrylate) (PBA) as a function of temperature. Some side-chain carbons in PEA and PBA show minima in T_1^C. On the basis of these results, the motion of CH_3 carbons and the CH_2 carbons in the side chain can be accounted for by the superposition of mainly two motions. One involves internal rotation or torsional oscillation of each functional group. The other is a slower motion induced by backbone motion. In addition, a molecular dynamics (MD) trajectory of 1.0-ns duration has been computed for a methyl-terminated atactic poly(ethyl acrylate) at 80 °C. The results of the MD calculation were in general agreement with the results of ^{13}C spin–lattice relaxation.

1. Introduction

High-resolution NMR is a powerful tool for getting information about molecular motions of polymers. To gain a deeper insight into the chain motion, several investigators have measured NMR relaxation parameters, typically the ^{13}C spin–lattice relaxation time T_1^C, as a function of temperature on a number of amorphous polymers.[1-5] The experimental results have been analyzed in terms of molecular motions by using particular autocorrelation functions that correlate the relaxation parameters with dynamics of polymers.[6-17] In spite of the basic importance of the method, polymers probed by the NMR relaxation measurements have been rather limited. It is desirable to have data for a wider variety of polymers.

Polyacrylates are fundamental polymers and they are also industrially important as raw materials of oil-resistant rubbers. Detailed molecular-level studies, however, have not been plentiful for polyacrylates in the bulk state.[18-28] Matsuzaki et al. have already determined the stereochemical configurations by ^1H NMR[18] and ^{13}C NMR[19] spectra of several polyacrylates and model compounds in solvent. In contrast, the molecular motions have been studied by pulsed ^1H NMR[20,21] and dielectric[22,23] and dynamic mechanical[24-26] relaxation. ^{13}C spin–lattice relaxation measurements, which probe local motions of polymer chains, have not been reported to date.

In the past few years, molecular dynamics (MD) computer simulation has been emerging as a novel tool for the investigation of the structure and dynamics of amorphous polymers.[29-38] The atomistic MD method is especially useful for analysis of motional processes since it provides the entire atomic coordinates of polymers as a function of time. In regard to the NMR relaxation measurements the use of the MD method is very attractive because it is free from the arbitrariness that more or less plagues the conventional analysis by using autocorrelation functions. On the other hand, the applicability of the MD method is severely limited by the time scale it can cover. The recent progress in computer hardware, however, has made the atomistic MD method capable of pursuing molecular motions with correlation time τ_c of the order of 10^{-9} s, which can be detected by ^{13}C spin–lattice relaxation time measurements.

In the present paper, we report ^{13}C spin–lattice relaxation measurements observed for bulk poly(ethyl acrylate) (PEA) and poly(*n*-butyl acrylate) (PBA) over a wide temperature range. In addition, the experimental data are analyzed with a MD trajectory computed for PEA in the amorphous state. Thus the molecular motions of PEA and PBA are elucidated by combination of the NMR experiments and atomistic computer simulation. To the best of our knowledge, such combination is used for the first time in the present paper.

2. Experimental Section

2-1. Materials. PEA and PBA samples were prepared from purified ethyl acrylate and *n*-butyl acrylate by solution polymerization in methyl ethyl ketone with azobis(isobutyronitrile) and mercaptoethanol as initiator and chain transfer agent, respectively, at 55 °C for ca. 3 h. The polymers obtained were purified by reprecipitation into methanol as nonsolvent and dried in vacuum for at least 24 h at 25 °C.

The molecular weights were estimated by GPC at 35 °C with a flux of 1.0 mL/min of tetrahydrofuran. Polystyrene standards were used to calibrate the hydrodynamic volume. The obtained $\bar{M}_n$ and polydispersity index of PEA were 9.67×10^4 and 1.79, respectively. Those of PBA were 1.32×10^5 and 1.56, respectively. Both samples were found to be atactic with meso:racemic ratios of 45:55 as determined by 270-MHz ^1H NMR in solution. The glass transition temperatures of PEA and PBA were −20.3 and −51.9 °C, respectively, as determined by extrapolation to a heating rate of 0 °C/min using T_g values measured on a Perkin-Elmer DSC7 differential scanning calorimeter at two heating rates of 5 and 10 °C/min.

2-2. NMR Measurements. High-resolution solid-state ^{13}C NMR spectra and ^{13}C spin–lattice relaxation times T_1^C were measured on a JEOL GSX-270 pulsed FT NMR spectrometer at 67.8 MHz with a CP/VT probe. The chemical shifts relative to tetramethylsilane were determined from the CH resonance line (29.50 ppm) of solid adamantane at 25 °C. ^{13}C spin–lattice relaxation times were calculated using the inversion–recovery method modified by the pulse saturation transfer technique or the pulse sequence developed by Torchia[39] in the temperature range from −100 to +125 °C. The temperatures of the samples were obtained by calibration with ^1H chemical shifts of the OH group of methanol or ethylene glycol. The spinning speed was 5.2–5.8 kHz, and the spinners were made from zirconium oxide with a Vespel.

2-3. MD Computer Experiment. To facilitate the interpretation of the results from the NMR experiments, an MD trajectory of 1.0-ns duration was generated for a methyl-terminated atactic PEA. The simulated system was a single-

• Abstract published in *Advance ACS Abstracts*, November 1, 1993.

0024-9297/93/2226-7326$04.00/0

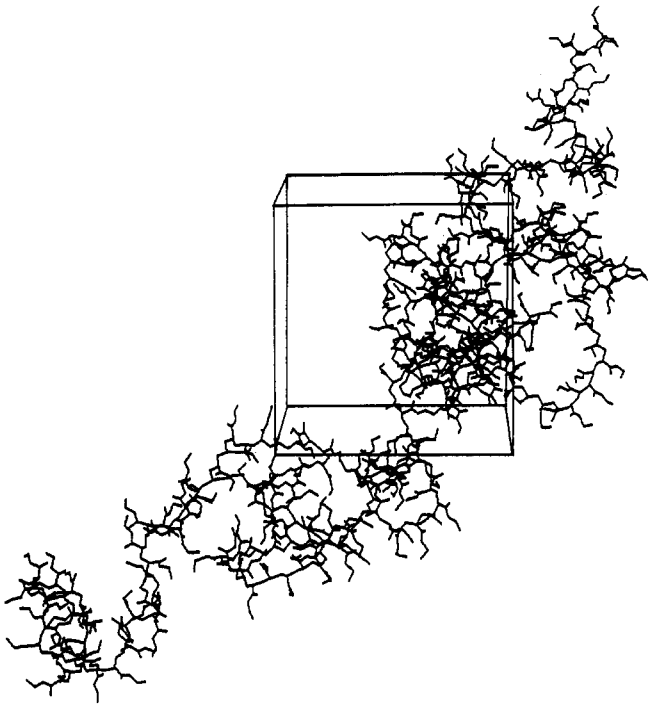

Figure 1. A typical PEA structure computed by the MD method with the cell-edge lengths being 36.1 Å on average.

chain PEA surrounded by its periodic images under the periodic boundary conditions. Figure 1 shows a typical snapshot of the MD trajectory. In Figure 1 the polymer is in a bulk state because its periodic images, which are not drawn in the figure, fill the vacant spaces. The molecular weight of the PEA chain is 30065, which corresponds to a polymerization degree of 300. The united-atom model was employed to reduce the computational load. The H atoms are therefore excluded, and the PEA chain has 2102 atomic centers. The tacticity of the PEA chain was set at the meso/racemic ratio of 44/56, which corresponds to a similar ratio of the real polymer used in the NMR measurements. The constant-temperature and constant-pressure MD method was used with the temperature and pressure set at 80 °C and 1 atm. The temperature 80 °C was chosen because it was a significant temperature observed in the NMR experiments.

The computational polymer sample was prepared initially at 20 °C by the MD run of 1.98-ns duration starting from a gaslike structure.[40] The temperature was then raised to 80 °C, and the dynamics was run for 1.25 ns. The trajectory of the last 1-ns MD run was used for the analysis. In the MD computation the time increment was 1 fs and the cutoff radius of the nonbonding forces was 7.5 Å. The calculated density of the polymer was 1.09 and 1.06 g/cm^3 at 20 and 80 °C, respectively, as compared to the experimental density at 25 °C of 1.12 g/cm^3.[41] Further technical details of the MD simulation are found elsewhere.[40]

According to the theory of NMR, the ^{13}C spin–lattice relaxation times are derived from the orientation autocorrelation functions associated with the C–H bond vectors. The autocorrelation functions K_i (i = 0,1,2) are defined as

$$K_i(\tau) = \langle Y_i(t+\tau)\, Y_i(t) \rangle \tag{1}$$

where

$$Y_0 = r^{-3}(1 - 3\cos^2\theta) \tag{2}$$

$$Y_1 = r^{-3}\sin\theta\cos\theta\exp(i\phi) \tag{3}$$

$$Y_2 = r^{-3}\sin^2\theta\exp(2i\phi) \tag{4}$$

with r, θ, and ϕ being general polar coordinates of the C–H bond vector.[42] The brackets in eq 1 mean the ensemble average.

On account of the use of the united-atom model C–H bond vectors were not immediately available out of the MD simulation. C_i–H vectors on a carbon atom C_i can be derived from C_i–X_α vectors, where X_α represents C or O atoms bonded to the C_i atoms. Let us denote the normalized C_i–X_α vectors as n_α (α = 1–3 for a methine carbon and α = 1,2 for a methylene carbon). The C_i–H vector on a methine carbon C_i was represented by

$$\vec{C_iH} = -r_{CH}\frac{n_1 + n_2 + n_3}{|n_1 + n_2 + n_3|} \tag{5}$$

The C_i–H vectors on a methylene carbon C_i were calculated by

$$\vec{C_iH} = r_{CH}\left(\frac{-n_1 - n_2}{|n_1 + n_2|}\cos\frac{\theta_{HCH}}{2} \pm \frac{n_1 \times n_2}{|n_1 \times n_2|}\sin\frac{\theta_{HCH}}{2}\right) \tag{6}$$

The constants r_{CH} and θ_{HCH} were taken to be 1.09 Å and 106.3°, respectively. Since the C–H vectors on a methyl carbon cannot be represented in a similar manner, $K_i(\tau)$ functions were not computed for methyl carbons.

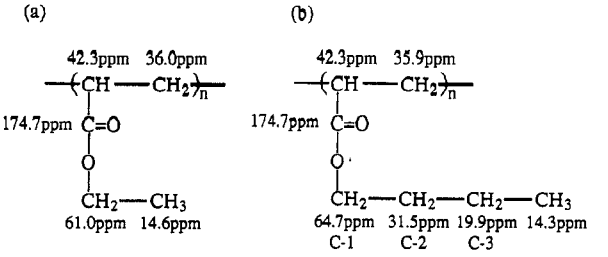

Figure 2. ^{13}C chemical shifts of polyacrylates in the solid state at 62 °C (in ppm relative to TMS): (a) PEA; (b) PBA.

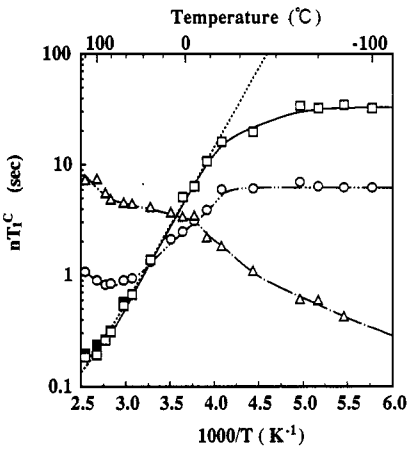

Figure 3. ^{13}C spin–lattice relaxation times nT_1^C at 67.8 MHz for the individual protonated carbons of bulk PEA as a function of inverse temperature, where n is the number of directly bonded protons: CH (□) and CH_2 (■) in the main chain of PEA; OCH_2 (○); CH_3 (△). The best fit of the experimental values for the main-chain carbons in the temperature range above the glass transition temperature with the assumption of isotropic rotation is shown as a dotted line.

3. Results and Discussion

3-1. NMR Relaxation Experiments. The ^{13}C PST-MAS spectra of bulk PEA and PBA measured at 62 °C show five peaks and seven peaks, respectively. Their assignment is given in Figure 2. There is partial overlap of the peaks corresponding to the CH and CH_2 carbons. The overlap increases at lower temperatures, making the relaxation measurement less accurate.

Figure 3 shows the measured nT_1^C, where n is the number of directly bonded protons, as the function of the reciprocal of temperature for each type of carbon in bulk PEA. An nT_1^C minimum is clearly observed at 80 °C for the CH_2 carbon in the side chain. Since the nT_1^C minimum occurs at $\omega\tau_c \approx 1$, the correlation time τ_c of molecular motion is on the order of $1/\omega \approx 10^{-9}$ s, with the Larmor frequency ω of $2\pi \times 67.8$ MHz in the present measurement. The nT_1^C of the main-chain carbons and the CH_3 carbon may have minima outside the measurement range, at a higher temperature for the former and at a lower temperature

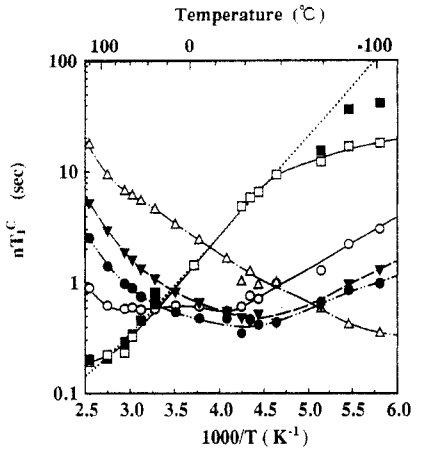

Figure 4. ^{13}C spin–lattice relaxation times nT_1^C at 67.8 MHz for the individual protonated carbons of bulk PBA as a function of inverse temperature, where n is the number of directly bonded protons: CH (□) and CH_2 (■) in the main chain; C-1 (○), C-2 (●), C-3 (▼), and CH_3 (△) in the side chain. The best fit of the experimental values for the CH carbon in the temperature range above the glass transition temperature with the assumption of isotropic rotation is shown as a dotted line.

for the latter. From the temperatures at which the minima occur, one may compare the local molecular mobility of the CH_3 carbon, side-chain CH_2 carbon, and main-chain carbons. Their mobilities decrease in that order.

Figure 4 shows the behavior of nT_1^C for bulk PBA. Like the case of PEA, the nT_1^C curve of the CH_3 carbon may have a minimum below the measured temperature range. Also, a minimum may appear for the main-chain carbons near or above 130 °C. On the other hand, broad minima of nT_1^C are actually observed for all of the CH_2 carbons in the side chain. These minima are broader than the minimum for the side-chain CH_2 of PEA. This observation indicates that the motion of the side chain of PBA is more complex than that of PEA. The minima for the C-2 and C-3 carbons in the butyl group occur at ca. −40 and −50 °C, respectively. The nT_1^C curves of C-2 and C-3 carbons are quite similar, indicating the similarity in the mobility of the two carbons. The most interesting phenomenon shown in Figure 4 is the appearance of double minima for the C-1 carbon of the butyl group at ca. 70 and ca. −30 °C. This subject will be discussed later in detail.

Figures 3 and 4 are all the data of our NMR experiments. What comes next are the analyses of the NMR data in terms of the motions of the polymer chain. Such analyses or interpretations are presented below separately for the backbone, side-chain, and methyl-group motions. The MD analyses are given in the last part of this section.

3-2. Backbone Motion. The conventional analysis was first made for the backbone carbons by using the isotropic reorientation model,[42] in which the correlation time τ_c is expressed as $\tau_c = \tau_{c0} \exp(\Delta E/kT)$. The best fit to the experimental nT_1^C values are shown as dotted curves in Figures 3 and 4. The apparent activation energy, ΔE, computed from the τ_c for the main-chain carbons of PEA is 6.5 kcal/mol, while that of PBA is 4.1 kcal/mol. However, as shown in Figures 3 and 4, discrepancy occurs in the temperatures region close to the nT_{1C} minimum. This discrepancy indicates that the isotropic reorientation model is not sufficient to account for the backbone motions of PEA and PBA and that some anisotropic processes are present. Hence, the apparent activation energies obtained should be regarded as a qualitative estimate.

It has been generally accepted that the values of nT_1^C of polymer chains cannot be adequately explained by the isotropic reorientation model even in solution. Models of chain dynamics which consider anisotropic reorientations have been proposed by several investigators. Those models include the model of log χ^2 distribution by Schaefer,[15] three-correlation time theory by Howarth,[12,13] and Jones–Stockmayer three-bond jump theory.[7,8] However, observation of a minimum in nT_1^C is usually required to apply those models. Since nT_1^C minima have not been observed for main-chain carbons of both polymers, analyses beyond the isotropic reorientation model had to be given up.

It is worth noting that the slope of nT_1^C against $1/T$ for the backbone carbons of PBA is gentler than that of PEA. This difference can be interpreted in two ways. One interpretation invokes the superposition of some elemental motions. If elemental processes exist on the backbone of each polymer, the processes should be almost the same between PEA and PBA because of their identical backbone structure. The nT_1^C curve should be governed by the temperature dependence of the correlation times of the processes. Thus, assuming several correlation times without a distribution in τ_c values, the PBA chain is more flexible than the PEA chain since a broader curve of ($1/T$ vs. nT_1^C) corresponds to the smaller apparent activation energy for the elemental motion with a correlation time τ_c of the order of 10^{-9} s.

Alternatively, another interpretation is possible based on a single elemental process with a distribution of correlation times. Considering a distribution in τ_c, an increase of the width of the distribution would broaden the nT_1^C minimum regardless of the shape of the distribution. This distribution width can be related to the number of degrees of freedom in the distribution of correlation times.[15] Assuming a larger distribution width leads to broadening of the nT_1^C curve as actually observed for the main-chain carbons of PBA in Figure 4. The backbone motion of the PBA chain is therefore characterized, possibly, by more degrees of freedom than that of the PEA chain. In other words, the PBA chain is more flexible than the PEA chain.

Accordingly, the gentler slope in the main-chain nT_1^C curves of PBA relative to PEA reveals that the PBA chain is more flexible than the PEA chain, whether superposition of more than one elemental motion is assumed or a distribution in the correlation times is assumed. This conclusion is in accord with the relative order in the glass transition temperatures of the two polymers.

3-3. Side-Chain Motion. Conventional analysis using the isotropic reorientation model is of little value for the understanding of side-chain motions as exhibited in Figures 3 and 4. First, extremely broad minima observed for all the side-chain CH_2 carbons of PBA are far different from the usual behavior expected from the model. Furthermore, for the side-chain CH_2 carbons of both PEA and PBA, the nT_1^C value at the minimum is much higher than the value expected from the isotropic reorientation model. The model predicts that the nT_1^C minimum is ca. 0.1 s for the present frequency of 67.8 MHz, while the experimental nT_1^C minima for the side-chain CH_2 carbon of PEA and the C-1, C-2, and C-3 carbons of PBA are 0.8, 0.55, 0.4, and 0.43 s, respectively.

The high nT_1^C value at the minimum is difficult to explain by more elaborate models which assume a distribution in correlation times. An orientation autocorrelation function with a log χ^2 distribution has been proposed by Schaefer.[15] The normalized log χ^2 distribution function is written in terms of a variable s which is a b-base logarithmic function of τ:

$$F(s) = (1/\Gamma(p))(ps)^{p-1}p \exp(-ps) \qquad (7)$$

$$s = \log_b[1 + (b-1)(\tau/\tau_0)] \quad (8)$$

where τ_0 is the average correlation time corresponding to the mean value of s, p is a width parameter whose inverse corresponds to the variance, σ^2, of the χ^2 distribution, and $\Gamma(p)$ is the Γ function of p. The distribution in terms of correlation times, $G(\tau)$, is defined by

$$G(\tau)\,d\tau = F(s)\,ds \quad (9)$$

The distribution function $G(\tau)$ with parameters of b = 1000 and p = 2 is extremely broad and corresponds to a distribution width in τ of several orders. Using this function, the expected value of the nT_1^C minimum is ca. 0.3 s, which is the maximum value of this model. Thus this model cannot explain the observed high nT_1^C minima. Although a distribution of correlation times may exist, the high values of nT_1^C at the minima and/or the broad curves of $1/T$ vs. nT_1^C strongly suggest that the motion of the CH_2 carbons consists of multiple elemental motions.

In the case of PBA, a reasonable speculation about the identity of the multiple motions is that the side-chain motion is made up of a superposition of the rapid torsional oscillations around the oxygen-(C-1) bond, the (C-1)–(C-2) bond, and the (C-2)–(C-3) bond within a conformation, plus rotations around these bonds corresponding to the conformation change of the side group. Backbone motion and rotation around the bond between the CH carbon in the main-chain and the carboxyl group should also contribute to the side-chain motion. The motion of the side-chain of PEA would be figured in a similar manner.

The above discussion is in accordance with previous studies in which the influence of superposition of elemental motions on measured nT_1^C was studied. Although there are a variety of models proposed, they lead to the common conclusion that the effect of an anisotropic fast process (for example, a rapid atomic fluctuation on a picosecond time scale as indicated by Levy and Karplus[43]) and a libration of limited but significant amount about the rest position results in an increase in the measured nT_1^C. The torsional oscillation within a conformation that is discussed in the preceding paragraph corresponds to the anisotropic fast process studied in previous works. The torsional oscillation is also one of the central subjects in the MD simulations to be described later.

The most interesting phenomenon concerning side-chain rotation is the appearance of double minima for the C-1 carbon of the butyl group of PBA at ca. 70 and ca. −30 °C. The double minima sharply indicate the existence of two kinds of motions. Since the locations of the nT_1^C minimum for the C-2 and C-3, −40 and −50 °C, respectively, are close to the nT_1^C minimum of the C-1 carbon at −30 °C, these three minima should be closely related. The motion characterized by these minima is probably a cooperative motion of the entire butyl group in PBA. Side-chain rotation and conformational changes within the butyl group are the candidates of the cooperative motion. The fact that the temperatures of the nT_1^C minima for the C-1, C-2, and C-3 carbons decrease in that order indicates that the mobility of the side-chain carbons increases with the distance, through the bonds, from the main chain. The order of mobility of carbon atoms can thus be understood from the standpoint of the degree of the motional restriction caused by the main chain.

The motion of the C-1 carbon related to the nT_1^C minimum at 70 °C is slower than the cooperative motion discussed above. Although the minimum corresponding to this slower motion seems to disappear for the C-2 and C-3 carbons in PBA, there is a possibility that a subtle minimum is buried at higher temperatures. In any case, the origin of the slower motion is obscure so long as just nT_1^C data are examined. In this regard the nT_1^C minimum of the PEA side-chain CH_2 carbon is interesting because its location, 80 °C, is close to the C-1 higher temperature minimum. It seems reasonable to speculate that the two minima are the manifestation of a common motional process. More discussion will be given in the MD subsection.

3-4. Methyl-Group Motion. As already discussed, it is likely from Figures 3 and 4 that the CH_3 carbons of both polymers have an nT_1^C minimum somewhere below −100 °C. The motions of the CH_3 carbons are therefore much faster than those of the other carbons. From a geometrical point of view, the dominant rapid motion of the CH_3 group is either the internal rotation around the C_3 axis or the side-chain rotation. Further discussion, however, would not be warranted at this time when only nT_1^C data are available.

A remarkable finding concerning the CH_3 carbon data is the apparent discontinuity or kink observed in the CH_3 curve of PEA at −20 °C. Interestingly, the temperature is close to the glass transition temperature. However, it seems unlikely that the anomaly is a reflection of the glass transition, because no other nT_1^C curves, including the CH_3 carbon of PBA, show anomalous behavior at each glass transition temperature. A more likely explanation is that a minor minimum is hidden in the CH_3 curve of PEA. That is, the CH_3 curve is regarded as the superposition of two curves, a minor-minimum curve and a dominant curve, of which the minor-minimum curve is reduced to the plateau observed in the temperature range between 0 and 60 °C in Figure 3. From this explanation it follows that a relatively slow motion with a correlation time of the order of 10^{-9} s exists in the CH_3 group of PEA above room temperature. Since a similar anomaly is not detected in the methyl group of PBA, the presumed slow motion is not a motion inherently associated with methyl groups.

3-5. MD Simulation. Analysis of the MD trajectory obtained for PEA provides further evidence for the interpretations described above. Figure 5 shows the computed orientation autocorrelation function K_0, eq 1 with i = 0, for each type of CH bond vectors. In Figure 5 the normalized function $K_0(\tau)/K_0(0)$ is plotted, and the normalized K_1 and K_2 functions were virtually the same as the normalized K_0 function. The disturbance of the curves noticed near τ = 1 ns in Figure 5 is due to statistical errors and has no physical significance.

In the case of the isotropic reorientation model, the orientation autocorrelation function is written as

$$K_i(\tau) = K_i(0)\exp(-|\tau|/\tau_c) \quad (10)$$

where

$$K_0(0) = {}^4/_5 r_{CH}^{-6}, \quad K_1(0) = {}^2/_{15} r_{CH}^{-6}, \quad K_2(0) = {}^8/_{15} r_{CH}^{-6} \quad (11)$$

and τ_c is the correlation time that is given by the slope of the semilogarithmic plot of the function. The semilogarithmic plot of the same K_0 function as in Figure 5 is presented in Figure 6. While the semilogarithmic plot of eq 10 yields a straight line, the curves in Figure 6 are not straight. Thus, the MD simulation gives the same conclusion as the NMR experiments: the motions in the tens of megahertz region are too complex to be described by the isotropic reorientation model.

As seen in Figures 5 and 6, there is a rapid initial decay of the correlation for all carbons in the first 1–2 ps. The corresponding correlation time, τ_{init}, obtained by the initial

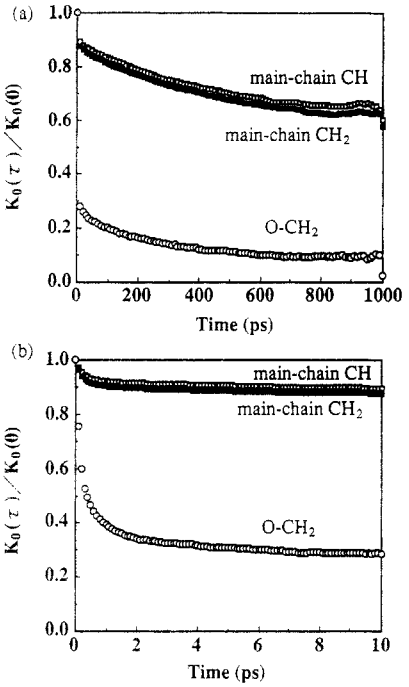

Figure 5. Normalized orientation autocorrelation function $K_0(\tau)/K_0(0)$ for each type of CH internuclear vector of atactic PEA obtained by MD simulation: (□) CH in the main chain; (■) CH_2 in the main chain; (○) CH_2 in the side chain. (a) The first 1 ns; (b) the first 10 ps.

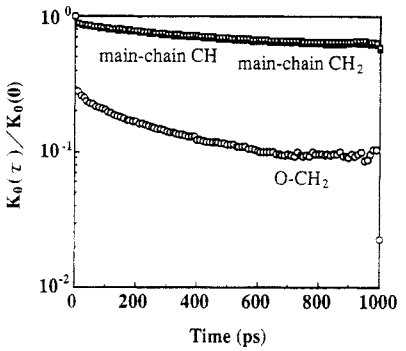

Figure 6. Semilogarithmic plots of the normalized orientation autocorrelation function $K_0(\tau)/K_0(0)$ displayed in Figure 5 during 1 ns: (□) CH in the main chain; (■) CH_2 in the main chain; (○) CH_2 in the side chain.

slope of the semilogarithmic plots of K_0 is 3.3 ps for the main-chain carbons. The initial decay is followed by a much slower loss of correlation over the rest of time. Therefore, the backbone motion is described by the superposition of at least two kinds of motions. One is a rapid motion on a picosecond time scale, while the other is dominant on a nanosecond time scale. Since the $K_0(\tau)/K_0(0)$ value for the main-chain carbons at 1 ns is ca. 0.6, which is much greater than $1/e$, it is concluded that the dominant slower motion of the main chain is characterized by a correlation time larger than 10^{-9} s at 80 °C. This conclusion is in agreement with the nT_1^C data of Figure 3, which indicates that the correlation time of the backbone carbon motion in PEA is larger than 10^{-9} s.

The τ_{init} value obtained for the side-chain CH_2 carbon from the corresponding semilogarithmic plot is 0.39 ps, which is an order of magnitude smaller than that of the main-chain carbon. The average correlation time, defined as the time at which $K_0(\tau)/K_0(0)$ becomes $1/e$, is ca. 1.4 ps for the side-chain CH_2 carbon. In other words, the initial rapid decay is the dominant decay process in the side-chain CH_2 motion. The dominant picosecond decay is followed by a much slower loss of correlation. The present

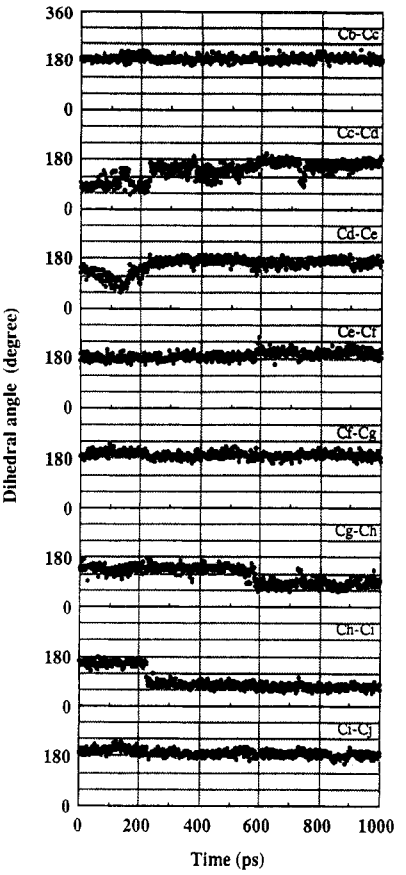

Figure 7. Typical trajectory of eight successive dihedral angles along the main chain, where subscripts on C indicate the carbons of the model shown in Figure 8.

MD analysis clarifies, at least partly, the questions in the interpretation of the nT_1^C curve of the side-chain CH_2 carbon in Figure 3. The nT_1^C minimum observed at 80 °C is ascribed to the slower decay process exhibited in Figures 5 and 6 because of the accordance in the time scale. The slower decay process can be approximated, though crudely, by using the correlation function of the isotropic reorientation model, eq 10. Since the initial picosecond decay makes the $K_0(\tau)/K_0(0)$ function drop to ca. 1/3 at the start of the slower decay (Figure 5), the preexponential factor of eq 10 has to be reduced to 1/3 of the proper isotropic reorientation model. Then the reduction of the preexponential factor causes an increase in the predicted nT_1^C minimum by a factor of 3.[43] Recalling the nT_1^C minimum of the proper isotropic reorientation model, 0.1 s, the present analysis gives the nT_1^C minimum of 0.3 s. Although discrepancy with the experimental value, 0.8 s, is still rather large, the MD analysis reveals a mechanism behind the observed high nT_1^C minimum.

It is difficult to determine the actual modes of motion using only T_1^C experiments. The merit of the MD simulation is that it can straightforwardly disclose these modes. To investigate the specific motion corresponding to each decay in the correlation, trajectories of dihedral angles were calculated from the MD trajectory of PEA. Eight successive main-chain dihedral angles at a particular part of the backbone are shown in Figure 7, where a dihedral angle of a trans conformation is defined as 180°. Figure 8 shows the schematic drawing of the segment of which the dihedral angles are shown in Figure 7 and subsequent figures. In Figure 7 two kinds of motions are clearly observed. One is rapid torsional oscillation around equilibrium angles with the amplitude of ca. 30°. The other is conformational jumps that occur at moderately long time intervals. It is remarkable that the conforma-

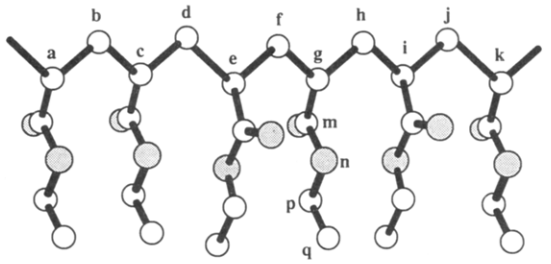

Figure 8. Schematic picture of the partial segment used for calculation of the trajectories of the dihedral angles of an atactic PEA, where the unshaded circles indicate carbon atoms and the shaded circles indicate oxygen atoms.

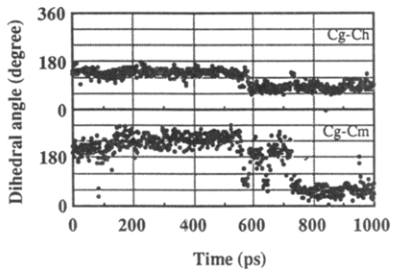

Figure 9. Trajectory of the dihedral angle C_f–C_g–C_h–C_i during 1 ns (upper plot) and trajectory of the dihedral angle C_f–C_g–C_m–O_n during 1 ns (lower).

tional jumps often occur synchronously or collectively over closely located monomer units, as seen clearly at ca. 220 ps and less clearly at ca. 570 ps. This type of motion is the so-called segmental motion. Occurrence of conformational change with a short rest period, as observed on the C_c–C_d bond at ca. 720 ps with the rest time of ca. 10 ps, is also interesting. It should be noted that conformations never changed during 1 ns at some segments. It seems possible that the frequency of the conformational jumps differs from segment to segment, producing a distribution in the corresponding correlation times. Though the present simulation time of 1 ns is too short, a length of 10 ns or so seems to be enough to examine the frequency distribution.

The features of the backbone motions discussed above should be shared by PBA, which has the same backbone structure as PEA. Results related to the backbone motion are now summarized fairly convincingly. The backbone motion which is responsible for the ^{13}C NMR spin–lattice relaxation for PEA and PBA involves the superposition of two main motions. One is a picosecond torsional oscillation within a given conformation. This type of motion corresponds to the rapid loss in the correlation K_i and causes a high value of nT_{1C}. The second motion is a segmental motion over a few monomer units, possibly with a distribution in its correlation time. The segmental motion leads to a slower decay of K_i and is responsible for the probable minimum in nT_1^C.

The trajectory of the dihedral angle C_f–C_g–C_m–O_n (see Figure 8) is shown in the lower half of Figure 9. The change of this angle involves rotation of the entire side chain. Features of the trajectory are similar to the backbone case in terms of the superposition of rapid torsional oscillation and an occasional conformational jump. The conformational jump seems to occur a little more frequently than that of the backbone. It is interesting that the motion seems to synchronize with the conformational jump of the C_g–C_h bond. This suggests that segmental motion of the backbone induces the side-chain rotation. Such a cooperative motion with the backbone certainly represents a slower mode of the side-chain motion. However, it must

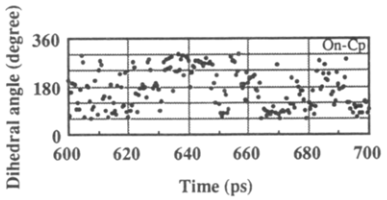

Figure 10. Typical trajectory of the dihedral angle C_m–O_n–C_p–C_q during 100 ps.

be pointed out that a slower motion of the side chain is also derived directly from the backbone motion.

Summarizing the side-chain motion, we conclude that the nT_1^C minima for the CH_2 carbon of the PEA side chain at 80 °C, the CH_3 carbon of PEA at 0–60 °C, and the C-1 carbon of the PBA side chain at 70 °C all result from segmental motion. It is worthy of discussion that there is a trend in the observed nT_1^C minima ascribed to the segmental motion. In Figure 3 the side-chain CH_2 minimum is clear, whereas the CH_3 minimum is obscure. The temperature of the minima lowers in order of the main-chain and side-chain CH_2 and side-chain CH_3 carbons. Therefore, the trend is the nT_1^C minimum becomes less clear and occurs at lower temperature as the position of the carbon gets further apart from the backbone. The same trend is recognized also in Figure 4 for PBA, in which the nT_1^C minimum due to the segmental motion disappears for the carbons that are further apart than C-1 from the backbone. The trend is naturally understood as the effect of increasing degrees of freedom with increasing number of bonds from the backbone, at which the segmental motion arises.

A trajectory of the torsional angle around the O_n–C_p bond (Figure 8) for 100-ps duration is shown in Figure 10. This motion is described as rapid torsional rotation that covers seemingly all accessible conformations. Obviously, this torsional rotation occurring on a picosecond time scale is the origin of the rapid and dominant loss in the K_0 function of the side-chain CH_2 carbon. As already explained, the rapid loss in the correlation function causes a high nT_1^C minimum. Since high nT_1^C minima are observed in PBA (Figure 4), the torsional rotation is very likely taking place in the side-chain of PBA, too. In Figure 3 the nT_1^C minimum corresponding to the torsional rotation is not observed in the measured temperature range. Thus, this nT_1^C minimum is expected to occur as a broad component in the temperature well below −100 °C.

4. Conclusions

In the present work, the dynamics of bulk PEA and PBA was investigated using ^{13}C spin–lattice relaxation experiments and MD simulations. We conclude the following:

(1) The backbone motions which are responsible for the ^{13}C NMR spin–lattice relaxations for PEA and PBA are described by the superposition of mainly two motions. One of the motions is a picosecond torsional oscillation within a stable conformation. The second is a segmental motion involving a cooperative conformational jump over a few monomer units. The correlation time of the segmental motion at ca. 120 °C is on the order of 10^{-9} s.

(2) The alkyl groups in the side chains of PEA and PBA rotate on a picosecond time scale above room temperature.

(3) The side-chain CH_2 carbon and CH_3 carbon of PEA and the C-1 CH_2 in the side chain of PBA move on a nanosecond time scale at 80, 0–60, and 70 °C, respectively.

These slower motions are related to segmental motions of the main chain.

(4) The results from the MD simulation generally agree with those from the T_1^C experiments with respect to the mobility of PEA. Thus, the simulated model is sufficiently correct to analyze the mobility qualitatively or semiquantitatively.

Acknowledgment. We express our appreciation to Professor Isao Ando for valuable discussions. We are also much indebted to Dr. Satoru Kuwajima (CRC Research Institute, Inc.) for support concerning MD simulations.

References and Notes

(1) Dejean de la Batie, R.; Laupretre, F.; Monnerie, L. *Macromolecules* **1988**, *21*, 2045; **1988**, *21*, 2052; **1989**, *22*, 122; **1989**, *22*, 2617.
(2) Laupretre, F.; Monnerie, L.; Virlet, J. *Macromolecules* **1984**, *17*, 1397.
(3) Gabrys, B.; Horii, F.; Kitamaru, R. *Macromolecules* **1987**, *20*, 175.
(4) Tanaka, H.; Gomez, M. A.; Tonelli, A. E. *Macromolecules* **1988**, *21*, 2934.
(5) Jo, Y. S.; Maruyama, Y.; Inoue, Y.; Chujo, R.; Tasaka, S.; Miyata, S. *Polym. J.* **1987**, *19*, 769.
(6) Heatley, F.; Begum, A. *Polymer* **1976**, *17*, 399.
(7) Jones, A. A.; Stockmayer, W. H. *J. Polym. Sci., Polym. Phys. Ed.* **1977**, *15*, 847.
(8) Jones, A. A.; Robinson, G. L.; Gerr, F. E. *ACS Symp. Ser.* **1979**, *No. 103*, 271.
(9) Tsutsumi, A.; Chachaty, C. *Macromolecules* **1979**, *12*, 429.
(10) Viovy, J. L.; Monnerie, L.; Brochon, J. C. *Macromolecules* **1983**, *16*, 1845.
(11) Valeur, B.; Monnerie, L. *J. Polym. Sci., Polym. Phys. Ed.* **1976**, *14*, 11.
(12) Howarth, O. W. *J. Chem. Soc., Faraday Trans. 2* **1978**, *75*, 863.
(13) Murayama, K.; Horii, F.; Kitamaru, R. *Bull. Inst. Chem. Res., Kyoto Univ.* **1983**, *61*, 229.
(14) Doddrell, D.; Glushko, V.; Allerhand, A. *J. Chem. Phys.* **1972**, *56*, 3683.
(15) Schaefer, J. *Macromolecules* **1973**, *6*, 882.
(16) Schneider, H. *J. Polym. Sci., Part B: Polym. Phys. Ed.* **1991**, *29*, 1171.
(17) McBrierty, V. J.; Douglass, D. C. *J. Polym. Sci., Macromol. Rev.* **1981**, *16*, 295.
(18) Uryu, T.; Shiroki, H.; Okada, M.; Hosonuma, K.; Matsuzaki, K. *J. Polym. Sci., Part A-1* **1971**, *9*, 2335.
(19) Matsuzaki, K.; Kanai, T.; Kawamura, T.; Matsumoto, S.; Uryu, T. *J. Polym. Sci., Polym. Chem. Ed.* **1973**, *11*, 961.
(20) Borisova, T. I.; Burshtein, L. L.; Shevelev, V. A.; Plate, N. A.; Shibaev, V. P. *Vysokomol. Soedin., Ser. A* **1973**, *15*, 674.
(21) Kawai, T. *J. Phys. Soc. Jpn.* **1961**, *16*, 1220.
(22) Murakami, I.; Ochiai, H.; Kodama, M.; Kubota, M. *Contemp. Top. Polym. Sci.* **1984**, *4*, 217.
(23) Gomez Ribelles, J. L.; Meseguer Duenas, J. M.; Monleon Pradas, M. *J. Appl. Polym. Sci.* **1989**, *38*, 1145.
(24) Sperling, L. H.; Tobolsky, A. V. *J. Polym. Sci., Part A-2* **1968**, *6*, 259.
(25) Chang, E. P.; Lin, K. S. C.; Bordoloi, B. K.; Kaelble, D. H. *16th National SAMPE Tech. Conf.* **1984**, 351.
(26) Tanaka, A.; Ishida, Y. *J. Polym. Sci., Polym. Phys. Ed.* **1975**, *13*, 431.
(27) Mathias, L. J.; Colletti, R. F. *Macromolecules* **1991**, *24*, 5515.
(28) Rutherford, H.; Soutar, I. *J. Polym. Sci., Polym. Phys. Ed.* **1977**, *15*, 2213.
(29) Rigby, D.; Roe, R. J. *Macromolecules* **1989**, *22*, 2259.
(30) Kremer, K.; Grest, G. S. *J. Chem. Phys.* **1990**, *92*, 5057.
(31) Murat, M.; Grest, G. S. *Macromolecules* **1989**, *22*, 4054.
(32) Takeuchi, H.; Okazaki, K. *J. Chem. Phys.* **1990**, *92*, 5643.
(33) Takeuchi, H.; Roe, R. J. *J. Chem. Phys.* **1991**, *94*, 7446; **1991**, *94*, 7458.
(34) Takeuchi, H.; Roe, R. J.; Mark, J. E. *J. Chem. Phys.* **1990**, *93*, 9042.
(35) Hutnik, M.; Gentile, F. T.; Ludovice, P. J.; Suter, U. W.; Argon, A. S. *Macromolecules* **1991**, *24*, 5962.
(36) Hutnik, M.; Argon, A. S.; Suter, U. W. *Macromolecules* **1991**, *24*, 5970.
(37) Boyd, R. H.; Pant, P. V. K. *Macromolecules* **1991**, *24*, 6325.
(38) Smith, G. D.; Boyd, R. H. *Macromolecules* **1992**, *25*, 1326.
(39) Torchia, D. A. *J. Magn. Reson.* **1978**, *30*, 613.
(40) Kikuchi, H.; Seki, K.; Kuwajima, S. *Macromolecules*, submitted for publication.
(41) Van Krevelen, D. W. *Properties of Polymers*; Elsevier: Amsterdam, 1976.
(42) Bloembergen, N.; Purcell, E. M.; Pound, R. V. *Phys. Rev.* **1948**, *73*, 679.
(43) Levy, R. M.; Karplus, M. *J. Am. Chem. Soc.* **1981**, *103*, 994.

Author Supplied Registry Nos. Poly(ethyl acrylate) (homopolymer), 9003-32-1; poly(*n*-butyl acrylate) (homopolymer), 9003-49-0.